

Morphogenesis as a Collective Decision of Agents Competing for Limited Resource: a Plants Approach

Payam Zahadat, Daniel Nicolas Hofstadler, and Thomas Schmickl

Artificial Life Lab, University of Graz, Graz, Austria
payam.zahadat@uni-graz.at

Abstract. Competition for limited resource is a common concept in many artificial and natural collective systems. In plants, the common resources – water, minerals and the products of photosynthesis – are a subject of competition for individual branches striving for growth. The competition is realized via a dynamic vascular system resulting in the dynamic morphology of the plant that is adapting to its environment. In this paper, a distributed morphogenesis algorithm inspired by the competition for limited resources in plants is described and is validated in directing the growth of a physical structure made out of braided modules. The effects of different parameters of the algorithm on the growth behavior of the structure are discussed analytically and similar effects are demonstrated in the physical system.

1 Introduction

Nature is full of patterns and forms. A huge diversity of natural patterns emerges from self-organization of several components interacting with each other and with their environment. Many patterns are regular repetitions of semi-identical units of forms, e.g. regular patterns on the outer skin of animals, or nonlinear non-equilibrium chemical oscillators, i.e., the Belousov-Zhabotinsky reaction [12, 4]. Such patterns can be described by self-organizing “Turing processes” [28, 23]. More complex patterns are usually multi-level hierarchies of forms. A mechanism of developing such complex structures in nature is morphogenesis—a generative process starting the system from single units and developing it into a complex organism as a result of interactions between several components of the system and the environment, driven by the laws of physics and chemistry and directed by encoded information in the genome [12]. The wide diversity of patterns in both natural and artificial developmental systems and their inherent adaptivity to environmental conditions are investigated by many researchers [12, 4, 33]. Various models of developing systems have been introduced and used for artificial systems. One example are L-systems [22] which are abstract generative encodings devised to describe development of multicellular organisms, particularly plants. Variations of the model are used in developing structures of artificial organisms [16, 26]. Other examples of morphogenesis are models that are inspired

by cells, i.e. cell types and division, gene regulatory networks, and diffusion [10], or cellular automata with different types of cells [19].

A related area of research dealing with the development of complexity from local interactions is the field of multi-agent systems. Multi-agent systems span from swarm intelligence [2] that is widely inspired from social insects, to swarm robotics [14, 11, 34] and to distributed approaches in microeconomics and market-based methods [7, 6, 20]. A common subject of interest in all systems is the distribution of resources including distribution of labor [2, 30, 17, 29]. Individual agents in a swarm consume or contribute to common resources available for the swarm while pursuing their personal motivations. Having to share resources imposes dependencies between agents and thus the mechanisms of resource distribution can steer the behavior of the swarm in various ways. Such mechanisms are widely investigated in microeconomics and market-based control [6, 20]. The mechanisms of division of labor and task allocation in swarm intelligence and swarm robotics share similar challenges, e.g. how to distribute the agents as the limited resource to handle sets of given tasks [3, 18, 30].

Here we use a morphogenesis algorithm called Vascular Morphogenesis Controller (VMC) [32] which is inspired by distribution of common resources between branches of a plant by means of vascular dynamics. The algorithm acts based on competition of individual agents and via local interactions. The negative feedback mechanisms due to scarcity of resources for the branches and positive feedback loops reinforcing vessels that transfer resources to the favorable paths govern the dynamics of the growing system. The result is a dynamic system of vessels that allows exploration of the environment and leads to stronger pathways of common resource between the root and the tips located in more favorable regions of the environment. The concept has strong similarities with other swarm systems of self-organized path formation, e.g. the formation of pheromone trails connecting the nest of ants to patches of foods [8] which has inspired optimization algorithms [9] and is implemented in many robotic swarms (e.g., [5, 24, 27]).

This work is in the context of the project *flora robotica* [13] that explores the symbiosis between plants and artificial structures for developing adaptive bio-hybrid architectural artifacts. The VMC is used as an embodied distributed algorithm reflecting environmental features in directing the growth of the artificial structures. The growth process is realized here manually by adding new modules to the structure based on the collective decision of the distributed controller. However the process is reversible meaning removal of modules is also possible. As a method of additive construction of artificial structures, the old technique of braiding is used. The braids consisting of reciprocally interwoven filaments possess attributes of flexibility of topology and are well-suited for incorporation of wires and distributed electronics.

In the following, a general formulation of the VMC algorithm is introduced and the effects of parameters in the morphogenesis behavior of the structures are described following a formal approach. The parameter effects are then demonstrated in a set of experiments with physical structures built out of braided modules hosting sensors and VMC controllers.

2 The Model: Vascular Morphogenesis Controller

Vascular Morphogenesis Controller (VMC) is inspired by the mechanisms of growth and branching in plants. Individual branches in a plant act as agents of a swarm competing with each other for shared resources. Each branch explores its local environment and according to the modality of the local resources in the environment (e.g., light) it produces amounts of a hormone, called auxin [21]. The hormone flows root-wards and adjusts the quality of the vessels along its way. The vascular system of a plant is responsible for distributing essential resources (e.g., water and minerals) from the roots to all the branches. According to the *canalization* hypothesis [25, 1], a well-positioned branch (wrt. environmental resources, i.e., light) produces high amounts of auxin which leads to better quality of vessels and therefore more share of the common resources and ultimately more growth for the branch. The larger share of the resource for well-positioned branches means lower shares being distributed among the others. The growth of a well-positioned branch can locate it in even better regions of the environment and gives it more new branches which leads to a positive feedback loop of auxin production and growth. The collective decision making process enables the plant to find the favorable regions of the environment and to benefit the growth in those regions.

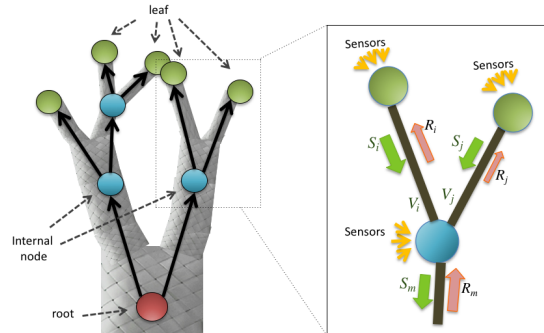


Fig. 1. An example structure guided by VMC. A value, called Successin, is produced at the leaves based on the sensor values and encoded parameters in the genome and flows root-wards through the internal nodes. The flow is modified at those nodes based on sensor values and parameters. The Successin flow adjusts the thickness of vessels which in turn are responsible for distributing the common resource from the root.

The VMC abstracts the above mentioned dynamics by introducing the growth process of acyclic directed graphs. Fig. 1 shows a schematic representation of VMC. The figure shows the flow of a value, we call Successin in analogy to auxin in a plant, produced at the leaves of the graph and propagating towards the root. The flow of Successin (S) regulates the thickness of vessels (weights of the edges of the graph). A common Resource (R) starts at the root and is

distributed between the children of each node proportional to their vessel thickness (V). Growth happens at the leaves by adding new nodes.

Similar to production of auxin in growing tips of plants, Successin is produced at the leaves (of the VMC graph) based on the local sensory inputs and constant parameters:

$$S_{leaf} := \text{PRODUCTION}(\text{params}, \text{sensors}) \quad (1)$$

Successin flows towards the root. At an internal node i , the flow of Successin is influenced by the inputs from the local sensors and constant parameters via a transfer function in the range of $[0, 1]$:

$$S_{\text{non-leaf}} := \text{TRANSFER}(\text{params}, \text{sensors}) \sum_{b \in \text{children}} S_b. \quad (2)$$

The weight of each connection (i, j) (thickness of the vessel) is adjusted based on Successin passing the connection (vessel) and the parameters determining the competition rate between the siblings:

$$V_{i,j} := V_{i,j} + \alpha(S_j^{\beta_i} - V_{i,j}), \quad \text{with} \quad \beta_i = \text{COMPETITION}(\text{params}, \text{sensors}), \quad (3)$$

where $V_{i,j}$ is the connection between node i and its child node j . S_j is the Successin of node j flowing towards i .

The above mentioned functions are implemented in this work as follows. The production rate of the Successin at the leaves is defined as

$$\text{PRODUCTION}(\text{params}, \text{sensors}) = f(\omega_{\text{const}} + \sum_{s \in \text{sensors}} \omega_s I_s), \quad (4)$$

where $f(x) = \max(0, x)$, ω_{const} is the constant production rate of Successin at a leaf and ω_s is the sensor dependent production rate which is the coefficient determining the dependency of Successin production on the sensor input I_s .

The transfer rate of Successin passing a node is defined as

$$\text{TRANSFER}(\text{params}, \text{sensor}) = g(\rho_{\text{const}} + \sum_{s \in \text{sensors}} \rho_s I_s), \quad (5)$$

where ρ_{const} is a constant transfer rate, ρ_s is the sensor-dependent transfer rate for sensor s , and $g(x) = \max(0, \min(1, x))$.

The competition rate is defined as:

$$\text{COMPETITION}(\text{params}, \text{sensor}) = \beta_{\text{const}} + \sum_{s \in \text{sensors}} \beta_s I_s, \quad (6)$$

where β_{const} is the constant competition rate and β_s is the sensor-dependent competition rate for sensor s .

Each of the parameters above can be set to zero depending on the particular applications.

Resource distribution over the structure. common resource starts at the root and is distributed throughout the structure according to vessel thickness (weight of connections). A part of the resource, R_i , reaching node i can be consumed at

that node and the remaining is divided among its children proportional to the thickness of their vessels. A given child j with vessel thickness $V_{i,j}$ receives

$$R_j := (R_i - c) \frac{V_{i,j}}{\sum_{b \in \text{children}} V_{i,b}}, \quad (7)$$

where c is the constant consumption rate of the resource at a node and ‘children’ is the set of children of node i . c can be set to zero in order to use the resource only at the leaves (for growth). The common resource initiated at the root can be a constant value or a function of the environment and/or Successin that reaches the root from anywhere within the graph. In the current implementation, the R_{root} is fixed to a constant value.

Addition of nodes. When the graph grows at a leaf, a number of new leaves appear as the children of the old leaf. The decision about the occurrence of growth on a particular leaf follows a growth strategy based on the share of the common resource reaching the leaf. Different strategies can be used to make the growth decision. For example, one strategy is to use a threshold th_{add} on the value of resource at the leaves to determine whether or not they should grow. In this case, the consumption rate of the nodes (c) in relation to the amount of resource at the root (R_{root}) puts a constraint on the overall graph size. Another example strategy is to consider the resource at the leaves as the probability of growth. In the current implementation, the leaf with the maximum resource value is the candidate node to grow next.

Deletion of nodes. Leaves can be removed from the VMC graph following a deletion strategy based on the resource reaching the nodes. A threshold th_{del} can be used to decide on the deletion of a node’s children. For example, a leaf i can be removed if $R_i < th_{\text{del}}$. Another example strategy is to remove all the children of a node i if they are all leaves and the amount of the resource at the node i is below the threshold. In the implementation used in this work, there is no deletion of nodes.

3 A Closer Look on the Effects of Parameters

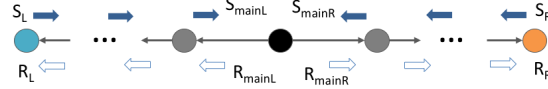
The parameters described in the previous section and their meanings are summarized in Table 1. Here we use a formal approach to look into the effect of some of these parameters.

Intrinsic tendency towards shorter paths A simplified 1-dimensional VMC structure is defined in Fig. 2. The root in this setup has two children and all the other nodes have a single child at most. The number of nodes between the leaves and the root on the left and the right side are n and m respectively. The sensor-dependent transfer and competition rates are set to zero ($\rho_s = \beta_s = 0$).

In a structure as in Fig. 2, the amount of Successin reaching the root from the left and right branches converge to $S_{\text{mainL}} = S_L \cdot \rho_c^n$ and $S_{\text{mainR}} = S_R \cdot \rho_c^m$

Table 1. List of parameters

parameter	description
α	adaptation rate of vessels
β_c	competition rate of sibling vessels, constant rate
β_s	competition rate of sibling vessels, sensor-dependent
ρ_c	transfer rate of Successin at the internal nodes, constant rate
ρ_s	transfer rate of Successin at the internal nodes, sensor-dependent
ω_c	production rate of Successin at the leaves, constant rate
ω_s	production rate of Successin at the leaves, sensor-dependent
c	consumption rate of resource in every node
R_{root}	constant resource value at the root

**Fig. 2.** An example 1-dimensional VMC graph

correspondingly. If the resource value at the root is $R_{\text{root}} = R$, and with the competition rate β_c , the vessel thicknesses for the branches of the root converge to $V_{\text{mainL}} = S_{\text{mainL}}^{\beta_c}$ and $V_{\text{mainR}} = S_{\text{mainR}}^{\beta_c}$ with a speed of α as the adaptation rate. The amount of the resource reaching each leaf converges to

$$R_L = R \frac{(S_L \rho_c^n)^{\beta_c}}{(S_L \rho_c^n)^{\beta_c} + (S_R \rho_c^m)^{\beta_c}} - n \cdot c, \quad R_R = R \frac{(S_R \rho_c^m)^{\beta_c}}{(S_L \rho_c^n)^{\beta_c} + (S_R \rho_c^m)^{\beta_c}} - m \cdot c, \quad (8)$$

In the case of $S_L = S_R$, the equations are simplified to

$$R_L = R \frac{\rho_c^{n\beta_c}}{\rho_c^{n\beta_c} + \rho_c^{m\beta_c}} - n \cdot c, \quad R_R = R \frac{\rho_c^{m\beta_c}}{\rho_c^{n\beta_c} + \rho_c^{m\beta_c}} - m \cdot c, \quad (9)$$

and therefore, the leaf with the shorter path to the root gets more of the resource. The preference for shorter paths is previously demonstrated in a case study of a maze scenario with a simulated VMC-controlled organism [31].

Regulation of growth in particular branches by using the sensor-dependent transfer rates. In the previous example, the transfer rate, ρ , was assumed to be identical in all nodes. However, the transfer rate can be also dependent on sensors (see Eq. 5). For instance, one can imagine a scenario with using light sensors influencing the production rate of Successin at the leaves, and accelerometers (providing the tilting angle of branches) or stress sensors (associated to physical joints) for influencing the transfer rate at the internal nodes. As an example, in the structure of Fig. 2, with $S_L = S_R$ and $m = n$ (see Eq. 9), a high stress or bending that influences an internal node at the left branch may decrease the ρ for that node and leads to $S_{\text{mainL}} < S_{\text{mainR}}$ and consequently $R_L < R_R$, which results in a preference for growth at the right branch.

Combined effect of the number of nodes, competition rate and transfer rate. Fig. 3 shows an example VMC graph with n children for each non-leaf node. Let's

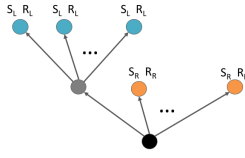


Fig. 3. An example VMC graph with n children for the root and its leftmost child.

assume that all the leaves of the left branch (represented in blue color) have the same sensor values and thus the same Successin production S_L , and all the other leaves (represented in orange color) also have the same Successin production, S_R . The ratio between the resources reaching a leaf at the left branch and one of the other leaves, depends on the ratio between their Successin values, as well as the competition and transfer rates and the value of n , and is computed as follows:

$$R_L = \frac{R_{\text{root}}}{V_{\text{sum}}} n^{\beta-1} (S_L \rho)^\beta, \quad R_R = \frac{R_{\text{root}}}{V_{\text{sum}}} S_R^\beta, \quad \implies \frac{R_L}{R_R} = n^{\beta-1} \rho^\beta \left(\frac{S_L}{S_R}\right)^\beta \quad (10)$$

where $V_{\text{sum}} = (n S_L \rho)^\beta + (n-1) S_R^\beta$ is the sum of all the vessels at the root node, R_L is the resource reaching a leaf of the left branch, and R_R is the resource reaching one of the other leaves.

In an environment with $S_L = S_R$, $\frac{R_L}{R_R} = n^{\beta-1} \rho^\beta$. This shows a potential tendency for growing children in branches that already hold larger number of nodes with large values of β and a potential tendency towards growing at the shorter branches with small values of ρ . The condition for the preference of the large branches is $n^{\frac{1-\beta}{\beta}} < \rho$. Considering that $\rho \leq 1$, the above condition never holds for $\beta \leq 1$.

4 Experiments with Physical Structures

Here we present a set of experiments representing the growth behavior of structures with various parameterizations. Most of the experiments are designed to demonstrate the parameter effects discussed in the previous section. The VMC is embodied in a set of controller nodes mounted on Y-shaped braided modules. A controller board is attached to the main part of the module, and two sensor boards, containing 4 light sensors and an accelerometer, are each attached to one of the branches. Each branch of a module can have a child module connected to it (see Fig. 4). The controller board maintains the communications with the children via the sensor boards and with its parent module. The detailed implementation of the modules are described in [15]. Each controller board contains a main VMC node. If a branch of a module has no child, the controller additionally keeps a leaf node associated to that branch. Otherwise, it adopts the main node of the child module as a child node of itself locating in a different module. This way, the VMC graph is formed and distributed over the structure. Growth of the structure is carried out by manually attaching a new braided module to the branch that contains the VMC leaf with the maximum resource value. Other

selection strategies could be used here (see *addition of nodes* in section 2), e.g. a threshold on the resource value at a leaf can determine whether or not the leaf should grow. Unless stated otherwise, in all the experiments here, the pa-

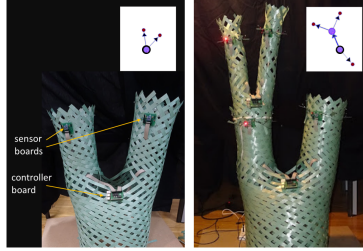


Fig. 4. An example braided module (left), and two connected modules (right), with their underlying VMC graphs (inset images). The circles with thick outline indicate the root nodes. The small circles are the leaf nodes associated with the branches of the modules with no child modules connected to them.

parameter settings are as follows: $\alpha = 0.9$, $\beta_c = 2$, $\rho_c = 0.5$, $\rho_{\text{tilt}} = 0.5$, $\omega_{\text{light}} = 1$, $R_{\text{root}} = 1$. All the other parameters are set to zero. The values from all the 4 light sensors are averaged and scaled to $[0, 1]$ to make the input variable I_{light} used in production of Successin at the leaf nodes. The value of the accelerometers indicating the tilting of the branches are also scaled to $[0, 1]$ to make the input variable I_{tilt} influencing the transfer rate at the internal nodes. Due to technical reasons regarding the communication protocol between the modules, the value of the Successin at all the leaves are rescaled with a factor of 0.167. In all the experiments $I_{\text{tilt}} \simeq 0.99$ unless stated otherwise.

Growing a structure with different competition rates. The effects of the competition rate β is investigated in this experiment with $\beta_c \in \{1, 2\}$ and with a light source at the top-left of the structure. Fig. 5 shows the growth of the braided structure with $\beta_c = 2$. At each step of the growth, a new module is added to the leaf branch with maximum resource among all the leaves. Fig. 6 shows the growth of the structure with $\beta_c = 1$. Since β_c cannot have any influence on the behavior of the first single module, we started the experiment with a second one already connected (step A in Fig. 5). As can be seen in the figures, the structure with larger competition rate grows strongly towards the brighter region of the environment while the other structure tends to grow all the branches with slight preference for the brighter region (see a video¹).

Combined effect of transfer rate and competition rate. The combined effect of transfer rate and competition rate are investigated here. The experiments are performed in room light (no directional light is used). The final structure from

¹ <https://youtu.be/-niKFhrXocI>

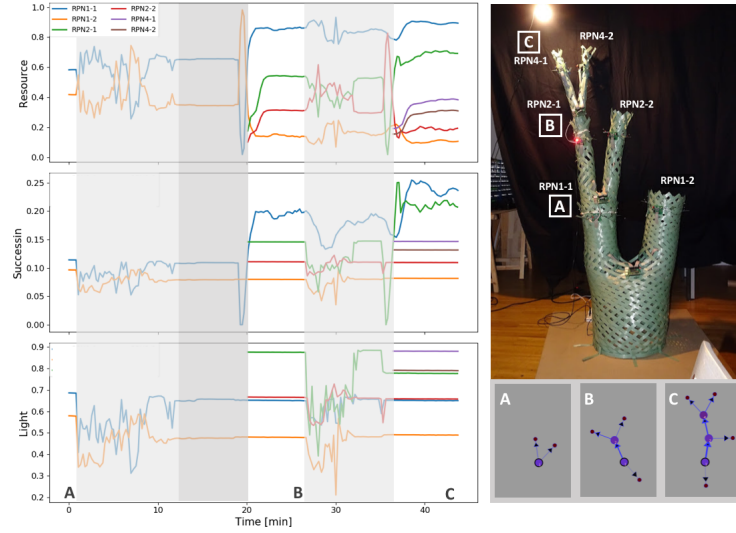


Fig. 5. The variables over the course of the growth (left) with $\beta = 2$, the final structure (right), and the VMC graphs of each growth step (bottom-right). The A-C labels in the plots mark the steps right before the start of manual growth. In the photo of the final structure, the labels indicate the position of the growth at each step. The shaded parts of the plots indicate the periods when the growth was physically realized.

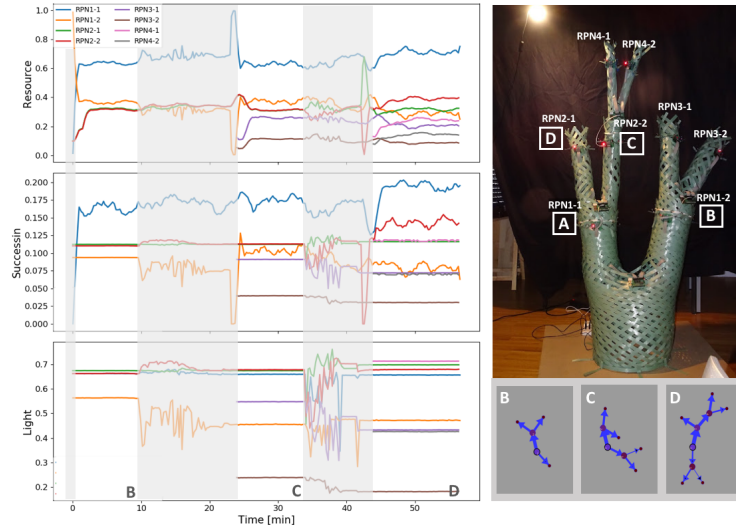


Fig. 6. The variables over the course of the growth (left) with $\beta = 1$, the final structure (right), and the VMC graphs of each growth step (bottom-right). The A-D labels in the plots mark the steps right before the start of manual growth. In the photo of the final structure, the labels indicate the position of the growth at each step. The shaded parts of the plots indicate the periods when the growth was physically realized.

Fig. 5 is used with $\rho_c \in \{0.25, 0.5\}$ and $\beta_c \in \{1, 2\}$. Considering that $\rho_{\text{tilt}} = 0.5$ and $I_{\text{tilt}} \simeq 0.99$, then $\rho = \text{TRANSFER} \in \{0.74, 0.99\}$. Table 2 shows the resource and the light value of each leaf, with the maximum resource value of each setup in bold and the maximum light values in italic fonts. The experiment shows a tendency towards shorter paths with smaller transfer rate and the tendency for further growth at the already grown branches with larger competition rate which is in line with the discussion in the previous section.

Table 2. Combined effect of competition and transfer rates.

ρ	β_c	State var.	1-2	2-2	4-1	4-2
0.99	2.0	Resource	0.112	0.227	0.364	0.287
		Light	0.806	<i>0.849</i>	0.787	0.698
0.99	1.0	Resource	0.252	0.268	0.247	0.219
		Light	0.809	<i>0.857</i>	0.793	0.702
0.74	1.0	Resource	0.358	0.279	0.189	0.168
		Light	0.806	<i>0.854</i>	0.791	0.699
0.74	2.0	Resource	0.231	0.289	0.263	0.205
		Light	0.804	<i>0.853</i>	0.791	0.698

Regulating growth in particular branches by using a sensor-dependent transfer rate. In this experiment the effect of sensor-dependent transfer rate is shown. The final structure of Fig. 5 is used in room light. After the first few minutes of the experiment with the intact structure, the leftmost branch is bent such that the I_{tilt} decreases considerably. Fig.7 shows the variable values over the course of the experiment. It shows that bending a branch leads to small values of I_{tilt} , decreases the transfer rate in the associated internal node and results in a lower share of resource for that branch which may eventually restrict its growth.

The effect of adaptation rate. In this experiment, the effect of different adaptation rates on the speed of dynamics of the system is investigated. A directional light source is located at the topleft of the structure. A cardboard is used to cast shades on the right branches in different time intervals in order to investigate the response time of the system to the shade/no-shade conditions. Two different adaptation rates $\alpha \in \{0.1, 0.9\}$ are tested. Fig. 8 demonstrates the variable values during the course of the experiments. It indicates slower changes in the resource values, reflecting slower change in the vessels, for the smaller α . Since the vessels act as a spatial memory for the system, the slow dynamics of the vessels can be beneficial in filtering out environmental noise.

5 Conclusion and Future Works

Morphogenesis of artificial structures is investigated here by using VMC, a recently introduced plant-inspired controller. The collective decision of the controller is based on the environmental and structural features and intrinsic properties of the controller determined by its parameters. The general formulation

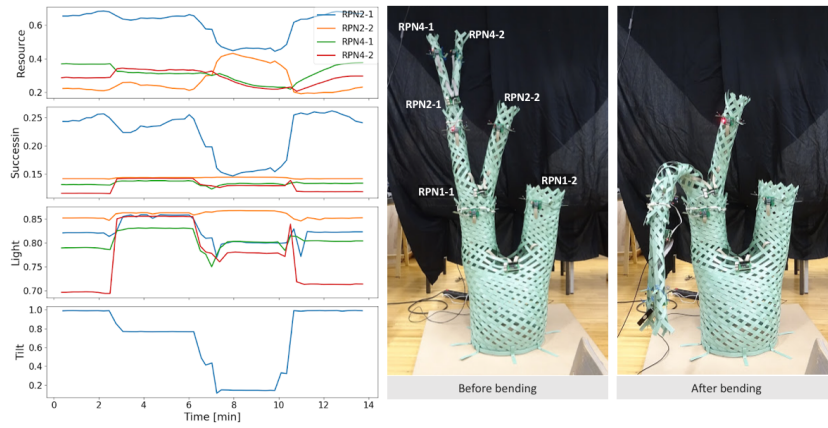


Fig. 7. Different variables in the course of the experiment with sensor-dependent transfer rate. The structure is first intact, then a branch is bent and then released again.

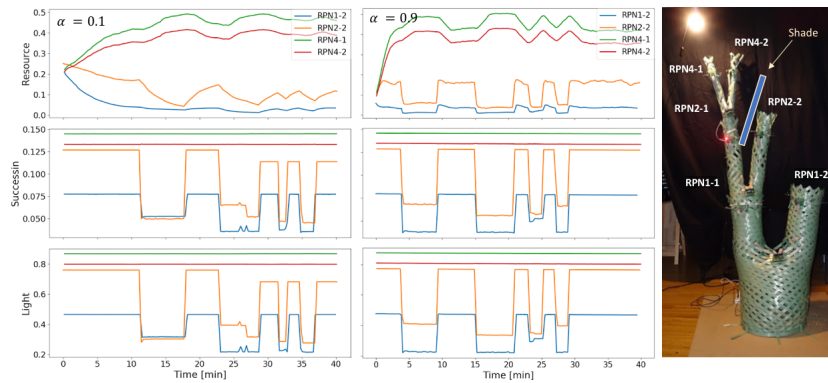


Fig. 8. The effects of small and large adaptation rates

of the algorithm is described here and the effects of some parameters are analytically discussed. The algorithm is validated by implementation in a physical braided structure. The parameter effects demonstrated by the physical structure follow the results of the formal analysis. In the future, other behaviors of the controlled system, e.g., the tendency towards asymmetry or dynamics of the structure (deletion and addition of nodes over time) will be investigated. Although the VMC has been so far only used in tree-like structures, nothing prevents the implementation on other acyclic directional graphs with several incoming connections to the nodes and several roots.

Acknowledgments. This work was supported by EU-H2020 project ‘florarobotica’, no. 640959.

References

1. Bennett, T., Hines, G., Leyser, O.: Canalization: what the flux? *Trends in Genetics* **30**(2), 41–48 (2014)
2. Bonabeau, E., Dorigo, M., Theraulaz, G.: *Swarm Intelligence: From Natural to Artificial Systems*. Oxford Univ. Press (1999)
3. Bonabeau, E., Sobkowski, A., Theraulaz, G., Deneubourg, J.L.: Adaptive task allocation inspired by a model of division of labor in social insects. In: *Biocomputing and emergent computation: Proceedings of BCEC97*. pp. 36–45. World Scientific Press (1997)
4. Camazine, S., Deneubourg, J.L., Franks, N.R., Sneyd, J., Theraulaz, G., Bonabeau, E.: *Self-Organizing Biological Systems*. Princeton Univ. Press (2001)
5. Campo, A., Gutiérrez, Á., Nouyan, S., Pinciroli, C., Longchamp, V., Garnier, S., Dorigo, M.: Artificial pheromone for path selection by a foraging swarm of robots. *Biological Cybernetics* **103**(5), 339–352 (Nov 2010)
6. Clearwater, S.H. (ed.): *Market-based Control: A Paradigm for Distributed Resource Allocation*. World Scientific Publishing Co., Inc., River Edge, NJ, USA (1996)
7. Deconinck, G., Craemer, K.D., Claessens, B.: Combining market-based control with distribution grid constraints when coordinating electric vehicle charging. *Engineering* **1**(4), 453 – 465 (2015)
8. Detrain, C., Deneubourg, J.L.: Self-organized structures in a superorganism: do ants behave like molecules? *Physics of Life Reviews* **3**(3), 162–187 (2006)
9. Dorigo, M., Maniezzo, V., Colnari, A.: Ant system: Optimization by a colony of cooperating agents. *Trans. Sys. Man Cyber. Part B* **26**(1), 29–41 (Feb 1996)
10. Doursat, R., Sánchez, C., Dordea, R., Fourquet, D., Kowaliw, T.: Embryomorphic engineering: Emergent innovation through evolutionary development. In: Doursat, R., Sayama, H., Michel, O. (eds.) *Morphogenetic Engineering*, pp. 275–311. *Understanding Complex Systems*, Springer Berlin Heidelberg (2012)
11. Ferrante, E., Turgut, A.E., Duenez-Guzman, E., Dorigo, M., Wenseleers, T.: Evolution of self-organized task specialization in robot swarms. *PLOS Computational Biology* **11**(8), 1–21 (2015)
12. Goodwin, B.: *How the Leopard Changed Its Spots: The Evolution of Complexity*. Princeton Univ Press (2001)
13. Hamann, H., Soorati, M., Heinrich, M., Hofstadler, D., Kuksin, I., Veenstra, F., Wahby, M., Nielsen, S., Risi, S., Skrzypczak, T., Zahadat, P., Wojtaszek, P., Støy, K., Schmickl, T., Kernbach, S., Phil, A.: *flora robotica* - An architectural system combining living natural plants and distributed robots. arXiv preprint arXiv:1709.04291 (2017)
14. Hamann, H.: *Swarm Robotics: A Formal Approach*. Springer (2018)
15. Hofstadler, D.N., Varughese, J.C., Nielsen, S.A., Leon, D.A., Ayres, P., Zahadat, P., Schmickl, T.: Artificial plants - vascular morphogenesis controller-guided growth of braided structures. arXiv preprint arXiv:1804.06343 (2018)
16. Hornby, G.S., Pollack, J.B.: Body-Brain Co-evolution Using L-systems as a Generative Encoding. In: *Proceedings of the Genetic and Evolutionary Computation Conference (GECCO-2001)*. pp. 868–875. Morgan Kaufmann, San Francisco, California, USA (Jul–Nov 2001)
17. Huberman, B.A., Hogg, T.: Distributed Computation as an Economic System. *Journal of Economic Perspectives* **9**(1), 141–152 (Winter 1995)

18. Karsai, I., Schmickl, T.: Regulation of task partitioning by a "common stomach": a model of nest construction in social wasps. *Behavioral Ecology* **22**, 819–830 (2011)
19. Kowaliw, T., Banzhaf, W.: *Mechanisms for Complex Systems Engineering Through Artificial Development*, pp. 331–351. Springer Berlin Heidelberg, Berlin, Heidelberg (2012)
20. Kurose, J.F., Simha, R.: A Microeconomic Approach to Optimal Resource Allocation in Distributed Computer Systems. *IEEE Trans. Comput.* **38**(5), 705–717 (1989)
21. Leyser, O.: Auxin, self-organisation, and the colonial nature of plants. *Current Biology* **21**(9), R331–R337 (2011)
22. Lindenmayer, A.: Developmental algorithms for multicellular organisms: A survey of L-systems. *Journal of Theoretical Biology* **54**(1), 3–22 (1975)
23. Murray, J.D.: On the mechanochemical theory of biological pattern formation with application to vasculogenesis. *Comptes Rendus Biologies* **326**(2), 239–252 (February 2003)
24. Payton, D., Daily, M., Estowski, R., Howard, M., Lee, C.: Pheromone robotics. *Autonomous Robots* **11**(3), 319–324 (Nov 2001)
25. Sachs, T.: The Control of the Patterned Differentiation of Vascular Tissues. *Advances in Botanical Research* **9**, 151–262 (jan 1981)
26. Sims, K.: Evolving 3D morphology and behavior by competition. In: Brooks, R., Maes, P. (eds.) *Artificial Life IV*. pp. 28–39. MIT Press (1994)
27. Sperati, V., Trianni, V., Nolfi, S.: Self-organised path formation in a swarm of robots. *Swarm Intelligence* **5**(2), 97–119 (Jun 2011)
28. Turing, A.M.: The chemical basis of morphogenesis. *Philosophical Transactions of the Royal Society of London. Series B, Biological Sciences* **B237**(641), 37–72 (1952)
29. Waldspurger, C.A., Hogg, T., Huberman, B.A., Kephart, J.O., Stornetta, S.: Spawn: A distributed computational economy. *IEEE Transactions on Software Engineering* **18**(2), 103–117 (1992)
30. Zahadat, P., Hahshold, S., Thenius, R., Crailsheim, K., Schmickl, T.: From honeybees to robots and back: Division of labor based on partitioning social inhibition. *Bioinspiration & Biomimetics* **10**(6), 066005 (2015)
31. Zahadat, P., Hofstadler, D.N., Schmickl, T.: Development of morphology based on resource distribution: Finding the shortest path in a maze by vascular morphogenesis controller. In: *14th European Conference on Artificial Life (ECAL-2017)*. vol. 14, pp. 428–429 (2017)
32. Zahadat, P., Hofstadler, D.N., Schmickl, T.: Vascular morphogenesis controller: A generative model for developing morphology of artificial structures. In: *Proceedings of the Genetic and Evolutionary Computation Conference*. pp. 163–170. GECCO '17, ACM, New York, NY, USA (2017)
33. Zahadat, P., Schmickl, T.: Generation of diversity in a reaction-diffusion-based controller. *Artificial Life* **20**(3), 319–342 (2014)
34. Zahadat, P., Schmickl, T.: Division of labor in a swarm of autonomous underwater robots by improved partitioning social inhibition. *Adaptive Behavior* **24**(2), 87–101 (2016)